Reaction of Trimethylchlorosilane in Spin-On Silicalite-1 Zeolite Film

ARTICLE *in* LANGMUIR · JUNE 2008

Impact Factor: 4.46 · DOI: 10.1021/la800086y · Source: PubMed

Reaction of Trimethylchlorosilane in Spin-On Silicalite-1 Zeolite Film

Salvador Eslava,[†,‡] Stephane Delahaye,[†] Mikhail R. Baklanov,[†] Francesca Iacopi,[†] Christine E. A. Kirschhock,[‡] Karen Maex,[†,§] and Johan A. Martens*[,‡]

IMEC, Kapeldreef 75, 3001 Leuven, Belgium, Centrum voor Oppervlaktechemie en Katalyse, Katholieke Universiteit Leuven, Kasteelpark Arenberg 23, 3001 Leuven, Belgium, and ESAT-INSYS, Katholieke Universiteit Leuven, Kasteelpark Arenberg 10, 3001 Leuven, Belgium

Received January 10, 2008. In Final Form: February 18, 2008

We present a study on the hydrophobization of spin-on Silicalite-1 zeolite films through silylation with trimethylchlorosilane. Microporous and micro-mesoporous Silicalite-1 films were synthesized by spin coating of suspensions of Silicalite-1 nanozeolite crystallized for different times. Ellipsometric porosimetry with toluene and water adsorbates reveals that silylation decreases the porosity and makes the films hydrophobic. The decrease in porosity depends on the exposed surface area in the pores. Water contact angle measurements confirm the hydrophobicity. Fourier transform infrared spectroscopy reveals that the trimethylsilyl groups are chemisorbed selectively on isolated silanols and less on geminal and vicinal silanols due to steric limitations. Time-of-flight secondary-ion mass spectroscopy and in situ ellipsometry analysis of the reaction kinetics show that the silylation is a bulk process occurring in the absence of diffusion limitation. Electrical current leakage on films decreases upon silylation. Silylation with trimethylchlorosilane is shown to be an effective hydrophobization method for spin-on Silicalite-1 zeolite films.

Introduction

Emerging applications of pure-silica-zeolite (PSZ) films cover a wide range of technologies such as separation processes,[1,2] chemical syntheses,[3] sensors,[4] and on-chip interconnects.[5,6] Especially, the MFI zeolite type known, e.g., as Silicalite-1 and ZSM-5 materials attracts a lot of attention.[7,8] Synthesis methods of Silicalite-1 films include in situ crystallization,[9] vapor-phase synthesis,[10] and spin-on coating.[5,6] The latter method consists of spinning on top of flat supports with a suspension of partially crystallized Silicalite-1 nanocrystals suspended in their synthesis liquor. The unconverted silica acts as a binder of the nanocrystals, improving the cohesion of the film.[11] The performance of PSZ films often depends on the hydrophobicity of the pore surfaces.[12] For instance, spin-on Silicalite-1 films used as low dielectric constant layers (low-*k*) in on-chip interconnects require hydrophobicity to avoid water uptake that would dramatically increase the dielectric constant.[13] Spin-on Silicalite-1 films are not hydrophobic enough for on-chip interconnects, even though Silicalite-1 micropores intrinsically are hydrophobic.[6] The problem arises from the presence of hydrophilic silanol groups on the external surfaces of the Silicalite-1 nanocrystals, on internal defects of the nanocrystals, and in the silica binder. A hydrophobization treatment, therefore, usually is necessary.

For hydrophobization of the surfaces of spin-on Silicalite-1 films, different approaches are possible. One approach involves the addition of methyltrimethoxysilane (MTMS) to the synthesis mixture for crystallizing the Silicalite-1 nanocrystals.[14] It results in the incorporation of $Si-CH_3$ moieties enhancing the hydrophobicity of the final Silicalite-1 film. Ultraviolet light-assisted curing effectively hydrophobizes spin-on Silicalite-1 films.[6] This treatment causes condensation of silanol groups and grafting of molecular fragments from the decomposition of the organic template. In UV-assisted curing, no reagents other than the entrapped synthesis template are needed to improve the hydrophobicity and the cross-linking of the crystallites composing the film. Silylation with trialkylsilane reagents is the most popular hydrophobization method.[15−19] On spin-on Silicalite-1 films, the silylation is performed after evacuation of the synthesis template.[5] The organic pore modification enhances the hydrophobicity. The commonly used silylation agent is trimethylchlorosilane (TMCS). It is preferred over other trialkylchlorosilanes because of its small molecular dimensions.

We investigated the silylation of spin-on Silicalite-1 films with TMCS. An extensive characterization of the Silicalite-1

* Corresponding author. E-mail: Johan.Martens@biw.kuleuven.be.
† IMEC.
‡ Centrum voor Oppervlaktechemie en Katalyse, Katholieke Universiteit Leuven.
§ ESAT-INSYS, Katholieke Universiteit Leuven.

(1) Algieri, C.; Bernardo, P.; Golemme, G.; Barbieri, G.; Drioli, E. *J. Membr. Sci.* **2003**, *222*, 181−190.
(2) Coronas, J.; Falconer, J. L.; Noble, R. D. *AIChE J.* **1997**, *43*, 1797−1812.
(3) McLeary, E. E.; Jansen, J. C.; Kapteijn, F. *Microporous Mesoporous Mater.* **2006**, *90*, 198−220.
(4) Grahn, M.; Wang, Z.; Lidstrom-Larsson, M.; Holmgren, A.; Hedlund, J.; Sterte, J. *Microporous Mesoporous Mater.* **2005**, *81*, 357−363.
(5) Wang, Z. B.; Mitra, A. P.; Wang, H. T.; Huang, L. M.; Yan, Y. S. *Adv. Mater.* **2001**, *13*, 1463−1466.
(6) Eslava, S.; Iacopi, F.; Baklanov, M. R.; Kirschhock, C. E. A.; Maex, K.; Martens, J. A. *J. Am. Chem. Soc.* **2007**, *129*, 9288−9289.
(7) Flanigen, E. M.; Bennett, J. M.; Grose, R. W.; Cohen, J. P.; Patton, R. L.; Kirchner, R. M.; Smith, J. V. *Nature* **1978**, *271*, 512−516.
(8) Kokotailo, G. T.; Lawton, S. L.; Olson, D. H.; Meier, W. M. *Nature* **1978**, *272*, 437−438.
(9) Wang, Z. B.; Yan, Y. S. *Chem. Mater.* **2001**, *13*, 1101−1107.
(10) Mizukami, F. *Stud. Surf. Sci. Catal.* **1999**, *125*, 1−12.
(11) Eslava-Fernandez, S.; Baklanov, M. R.; Iacopi, F.; Brongersma, S. H.; Kirschhock, C. E. A.; Maex, K. *Mater. Res. Soc. Symp. Proc.* **2006**, *914*, 0914-F03-08.
(12) Long, Y. C.; Jiang, H. W.; Zeng, H. *Langmuir* **1997**, *13*, 4094−4101.
(13) Maex, K.; Baklanov, M. R.; Shamiryan, D.; Iacopi, F.; Brongersma, S. H.; Yanovitskaya, Z. S. *J. Appl. Phys.* **2003**, *93*, 8793−8841.
(14) Li, S.; Li, Z.; Medina, D.; Lew, C.; Yan, Y. S. *Chem. Mater.* **2005**, *17*, 1851−1854.
(15) Zhao, X. S.; Lu, G. Q.; Whittaker, A. K.; Millar, G. J.; Zhu, H. Y. *J. Phys. Chem. B* **1997**, *101*, 6525−6531.
(16) Zhao, X. S.; Lu, G. Q. *J. Phys. Chem. B* **1998**, *102*, 1556−1561.
(17) Impens, N. R. E. N.; van der Voort, P.; Vansant, E. F. *Microporous Mesoporous Mater.* **1999**, *28*, 217−232.
(18) Sever, R. R.; Alcala, R.; Dumesic, J. A.; Root, T. W. *Microporous Mesoporous Mater.* **2003**, *66*, 53−67.
(19) Capel-Sanchez, M. C.; Barrio, L.; Campos-Martin, J. M.; Fierro, J. L. G. *J. Colloid Interface Sci.* **2004**, *277* (1), 146−153.

10.1021/la800086y CCC: $40.75
Published on Web 04/05/2008

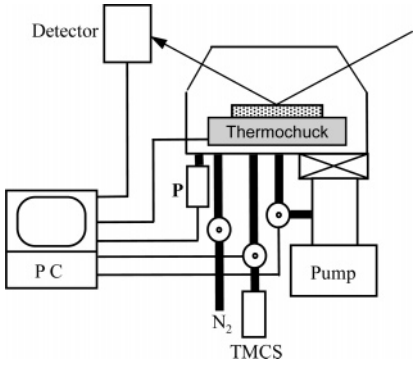

Figure 1. Schematic diagram of the unit used for the silylation of Silicalite-1 films with TMCS. The chamber is equipped with a spectroscopic ellipsometer (400−800 nm), a thermochuck, an ultrahigh vacuum pump, and a system for dosing gases.

films using ellipsometric porosimetry (EP) with different molecular probes, Fourier transform infrared spectroscopy (FT-IR), time-of-flight secondary-ion mass spectroscopy (TOF-SIMS), and contact angle determination provided insight into the silylation process. The influence of porosity in films prepared using Silicalite-1 suspensions crystallized for different times was investigated.

Experimental

Film Preparation. Spin-on Silicalite-1 films were synthesized following a procedure described by Wang et al.[5] First, in an autoclavable polypropylene bottle, the so-called *clear solution* was prepared using the following molar ratio of reactants: 2.8 TEOS/40 water/11.2 ethanol/1 TPAOH. TEOS (98%, Acros) and TPAOH (40%, Alfa-Aesar) stand for tetraethyl orthosilicate and tetrapropylammonium hydroxide, respectively. Note that 2.8 mol of TEOS produces 11.2 mol of ethanol by hydrolysis. A same quantity of ethanol relative to TEOS was added to the synthesis mixture. The mixture was aged for 3 days under stirring and then heated to 80 °C in an oil bath. During this hydrothermal treatment at 80 °C, Silicalite-1 nanocrystals nucleated and grew in suspension. After heating for 3, 4, and 4.5 days, the suspensions had different Silicalite-1 contents and crystal sizes. To remove dust and small amounts of large nanocrystals (>200 nm) ranging out of the targeted nanocrystal size below 100 nm, the Silicalite-1 suspensions were centrifuged at 5000 rpm for 30 min and subsequently filtered through 200 nm poly(tetrafluoroethylene) (PTFE) filters. Monodisperse suspensions were obtained with an average particle size determined using dynamic light scattering of 37, 46, and 57 nm after 3, 4, and 4.5 days of crystallization, respectively. The full width at half-maximum (fwhm) of the lognormal particle size distribution was 28, 24, and 17 nm after 3, 4, and 4.5 days of crystallization, respectively. The Silicalite-1 nanocrystal yield was determined as follows. The suspension was diluted with water (×5) to lower the viscosity and then centrifuged at 18 000 rpm for 2.5 h at 20 °C. The deposited nanocrystals were recovered in ethanol, calcined in air at 600 °C for 5 h, and weighed. The supernatant liquid was evaporated, and the residue was calcined and also weighed. The yield of nanocrystals on a total solids basis was 6, 16, and 31 wt % after 3, 4, and 4.5 days of crystallization, respectively. For the preparation of films, filtered Silicalite-1 suspensions were spun onto 6 × 6 cm^2 pieces of Si-p wafer. Si-n^{++} wafers were used for capacitance measurements. The spinning velocity was 3300 rpm for 30 s. The acceleration was 1300 rpm/s. The films were dried at 80 °C overnight. Subsequently, they were calcined at 450 °C in air on preheated plates for 3 h. The film thickness was 350−400 nm.

Silylation. The films were introduced in a chamber equipped with a spectroscopic ellipsometer working in the range of 400−800 nm, a thermochuck, an ultrahigh vacuum pump, and a system for dosing gases (Figure 1). First, the chamber was degassed to ultrahigh vacuum (10^{-7} mbar), and the films were heated at 450 °C for 2−3 h (step 1). After the degassing, TMCS (>99% GC-grade, Sigma-Aldrich) vapor was introduced into the chamber up to a pressure of 2 mbar, and the reaction was performed at 450 °C (step 2). During the hydrophobization reaction, the ellipsometric angles Ψ and Δ were regularly measured over the 400−800 nm wavelength range. Termination of the reaction with TMCS was probed by the ellipsometric angles reaching constant values. The chamber was degassed to vacuum (step 3). This degassing step was considered to be finished when the ellipsometric angles reached constant values. Then, the degassing was interrupted. Subsequently, TMCS was introduced at a pressure of 5 mbar for a second silylation treatment (step 4). When the reaction was finished, the chamber was degassed and purged with a nitrogen gas flow of 200 mL/min (step 5). Finally the films were gradually cooled to room temperature.

Characterization. EP measurements using toluene and water as molecular probes were performed using a Sentech SE801 spectroscopic ellipsometer. The same instrument was also used to monitor TMCS chemisorption. The incident angle was fixed at 70°. The refractive index and the film thickness were determined by applying the Fresnel equation to a layer model that describes the system and approximates the measured values of Ψ and Δ.[21] The Lorentz−Lorentz theory describes the relation between the refractive indices and the material composition in a multicomponent system:[22−23]

$$\frac{n^2-1}{n^2+2}=\sum V_i\frac{n_i^{\,2}-1}{n_i^{\,2}+2} \qquad (1)$$

where n is the refractive index of the multicomponent system, V_i is the volume fraction of component i, and n_i is the refractive index of component i. Considering the porous coating as a binary system composed of porous zeolite and adsorbed species, the refractive index measured during the incorporation of a species i is directly related to its volume fraction V_i.

The mesopore size distribution of a PSZ film was derived from the toluene adsorption isotherm through application of the Kelvin equation in the pressure range where capillary condensation occurs. Details of the determination of the pore size distribution via this method were published elsewhere.[22−24] FT-IR (Biorad FTS-40) in N_2 atmosphere served to characterize the chemical bonds in the films. Spectra averaged over 64 scans were recorded in the region of 4000−400 cm^{-1} with 4 cm^{-1} resolution. The contact angle of a 1 μL drop of double deionized water on the film surface at 20 °C was determined from a picture recorded with a camera and fitting of the curvature with the Young−Laplace equation. The dielectric constant of the films at 100 kHz was measured by impedance analysis (HP4284A-LCR meter) in a metal−insulator−semiconductor (MIS)-type capacitor obtained by deposition of Al dots on top of the film. The carbon profile in films prepared with Silicalite-1 suspensions crystallized for 3 and 4.5 days was characterized by TOF-SIMS in negative ion detection mode. Spectra were acquired using a bunched 15 keV Ga^+ primary ion beam and probing an area 100 × 100 μm^2 in size.

Results and Discussion

Ellipsometric Porosimetry. Toluene adsorption isotherms on spin-on Silicalite-1 films before and after silylation are shown in Figure 2. Before silylation, the films prepared with Silicalite-1 suspensions crystallized for 3, 4, and 4.5 days showed a total toluene uptake of 34, 36, and 39% of the film volume, respectively. The porosity increased when the Silicalite-1 suspension spun

(20) Yuan, P.; Yang, D.; Lin, Z. Y.; He, H. P.; Wen, X. Y.; Wang, L. J.; Deng, F. *J. Non-Cryst. Solids* **2006**, *352*, 3762−3771.
(21) Azzam, R. M. A.; Bashara, N. M. *Ellipsometry and Polarized Light*; North-Holland: Amsterdam, Holland, 1977.
(22) Baklanov, M. R.; Mogilnikov, K. P.; Polovinkin, V. G.; Dultsev, F. N. *J. Vac. Sci. Technol., B* **2000**, *18*, 1385−1391.
(23) Eslava, S.; Baklanov, M. R.; Kirschhock, C. E. A.; Iacopi, F.; Aldea, S.; Maex, K.; Martens, J. A. *Langmuir* **2007**, *23*, 12811−12816.
(24) Baklanov, M. R.; Mogilnikov, K. P.; Yim, J. H. *Mater. Res. Soc. Symp. Proc.* **2004**, *812*, F5.4.1−4.6.

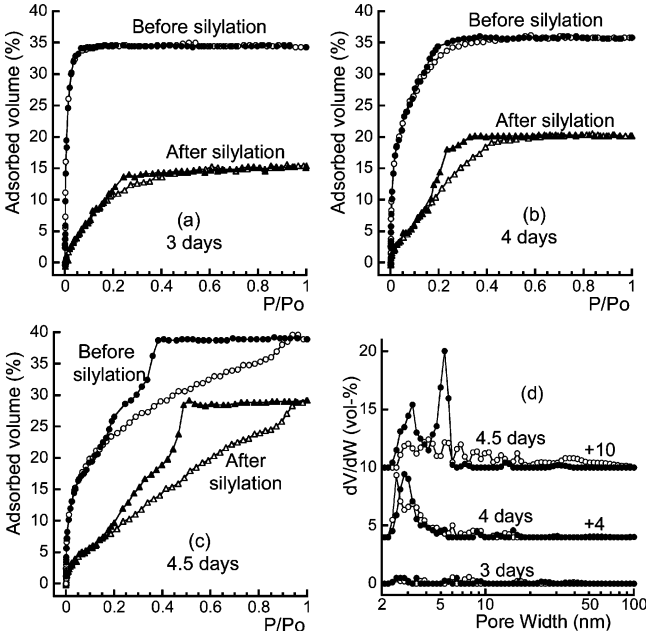

Figure 2. Toluene adsorption isotherms on spin-on Silicalite-1 films before and after silylation, measured by EP. The films were prepared using Silicalite-1 suspensions crystallized for different times: (a) 3 days, (b) 4 days, and (c) 4.5 days; (○,△) adsorption; (●,▲) desorption. (d) Pore size distribution in the range of 2−100 nm on spin-on Silicalite-1 films before silylation, calculated from the (○) adsorption branch and (●) desorption branch. Pore size distribution curves are vertically shifted over the indicated values (+4 for the 4 days film and +10 for the 4.5 days film).

onto the support was crystallized for a longer time. The film with 3 days crystallized Silicalite-1 was microporous (pore size < 2 nm) on the basis of the observation of a type I adsorption isotherm. Films prepared with Silicalite-1 suspensions crystallized for 4 and 4.5 days had both micropores (pore size < 2 nm) and mesopores (pore sizes 2−50 nm) because the isotherm was a convolution of a type I and a type IV isotherm.[25] Figure 2d shows the pore size distribution in the range of 2−100 nm derived from toluene adsorption isotherms. The film with 3 days crystallized Silicalite-1 contained little mesopores. In the films prepared using longer crystallized Silicalite-1 suspensions, mesopores were present. The pore size distribution was broader when the spun-on Silicalite-1 suspension was crystallized for 4.5 compared to 4 days. The reason for this broadening is the increase with crystallization time of the nanocrystal content and the decrease of residual silica serving as the binder. In such films there are more and/or wider interstitial voids between the nanocrystals. The investigated set of films covers the different porosities that can be encountered with spin-on Silicalite-1 films.

After silylation, the toluene uptake was lower in all films, indicating a decrease in porosity. After silylation, compared to the individual parent films, the porosity was 56, 44, and 26% lower, respectively (Figure 2). This reduction in porosity indicates that trimethylsilyl (TMS) groups partially fill the pore volume upon silylation. Since the decrease in toluene uptake coincided with an increase in refractive index (discussed below), the silylation occurred inside the film and did not merely limit the pore accessibility. The reduction of porosity was less pronounced in films with mesopores (4 and 4.5 days of crystallization). This can be understood considering that the coverage with TMS groups occurs through chemisorption on silanol groups located on pore

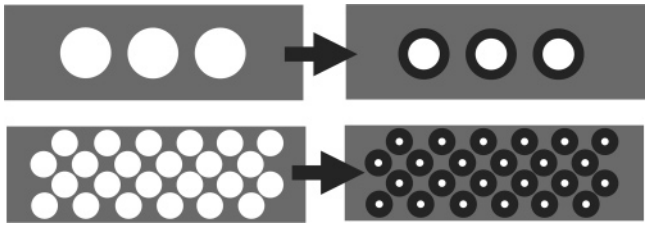

Figure 3. Porosity changes upon silylation (dark pore wall coating) of two films with the same initial pore volume but different pore sizes.

walls. The surface area of a film increases with porosity and decreases with the pore size. In the investigated set of films, the total porosity increased with the crystallization time of the Silicalite zeolite by ca. 5% (Figure 2a−c, toluene capacities before silylation). The pore size distribution abruptly broadened up to a few tens of nanometers when the Silicalite-1 was crystallized for 4.5 days (Figure 2). Films with large pores have a smaller surface area and a lower capacity for incorporation of TMS groups, as sketched in Figure 3.

Silylation caused an increase of the pressure at which toluene filled the film (Figure 2). This shift to higher pressures for capillary condensation was not expected to occur because of the expected decrease in effective pore width after the pore walls are coated with TMS (Figure 3).[18] However, the pressure at which capillary condensation occurs according to Kelvin's law depends on the pore shape and the surface tension as well.[25] Probably, the pore surface covered by TMS groups next to toluene had a lower surface tension compared to pore walls covered with a film entirely composed of toluene. A similar upward shifting of the pressure for capillary condensation has been observed in benzene adsorption on silylated MCM-41 material.[16]

The water adsorption isotherms on the three spin-on Silicalite-1 films before and after the TMS modification are shown in Figure 4. These water adsorption isotherms reveal the hydrophilicity of the pore surface of the parent films permitting the adsorption of water.[6,23,26] Water is physisorbed on silica surfaces through hydrogen bonding with silanol groups.[25,27,28] Water chemisorption causing hydrolysis of siloxane bonds can be recognized by strong hysteresis in the water adsorption isotherm.[23] Prior to silylation, all the films adsorbed more than 25% of water (Figure 4). The isotherms did not show hysteresis, suggesting that the films were hydrophilic and that water was adsorbed physically. After silylation, the shape of the water adsorption isotherms still did not suggest chemisorption. The water uptake was as low as a 4−5%. These water adsorption isotherms on silylated films revealed that, through silylation, the pores of the films had become hydrophobic. Thus, the concentration of hydrophilic centers was effectively decreased. The contact angle of water on top of the unmodified films was about 10°. After silylation, it raised to ca. 105°, 110°, and 115° for films with Silicalite-1 zeolite crystallized for 3, 4, and 4.5 days, respectively. The large water contact angle confirmed the hydrophobization.

The hydrophobization of spin-on Silicalite-1 films was repeated 10 times and was found to be very reproducible. The use of an even lower temperature during the silylation reaction (e.g., 300 °C instead of 450 °C) also effectively decreased the maximum water adsorption capacity to less than 8 vol %. The thermal stability and the aging of hydrophobized films were evaluated

(25) Gregg, S. J.; Sing, K. S. W. *Adsorption, Surface Area and Porosity*, 2nd ed.; Academic Press: London, England, 1982; Chapters 1, 3, and 5.

(26) Baklanov, M. R.; Mogilnikov, K. P.; Le, Q. T. *Microelectron. Eng.* **2006**, *83*, 2287−2291.

(27) Steiner, T. *Angew. Chem., Int. Ed.* **2002**, *41*, 48−76.

(28) Brinker, J.; Sherer, G. W. *Sol-Gel Science: The Physics and Chemistry of Sol-Gel Processing*; Academic Press: San Diego, CA, 1990; Chapter 10.

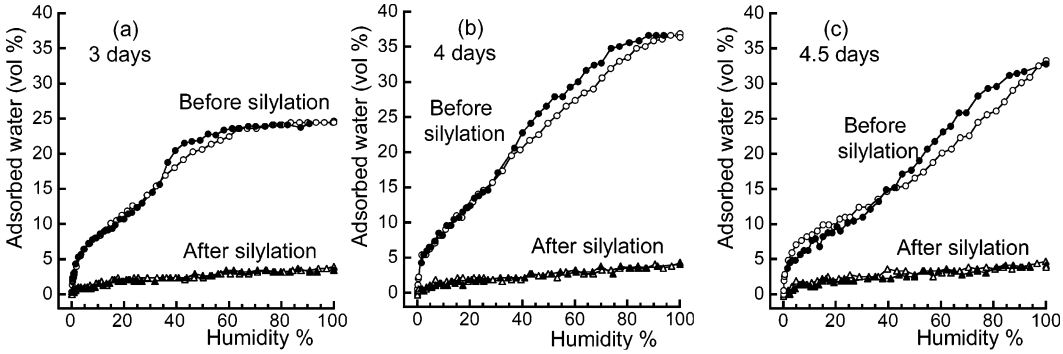

Figure 4. Water adsorption isotherms on spin-on Silicalite-1 films before and after silylation. The films were prepared using (a) 3 days, (b) 4 days, and (c) 4.5 days crystallized Silicalite-1 suspensions: (○&△) adsorption; (●,▲) desorption.

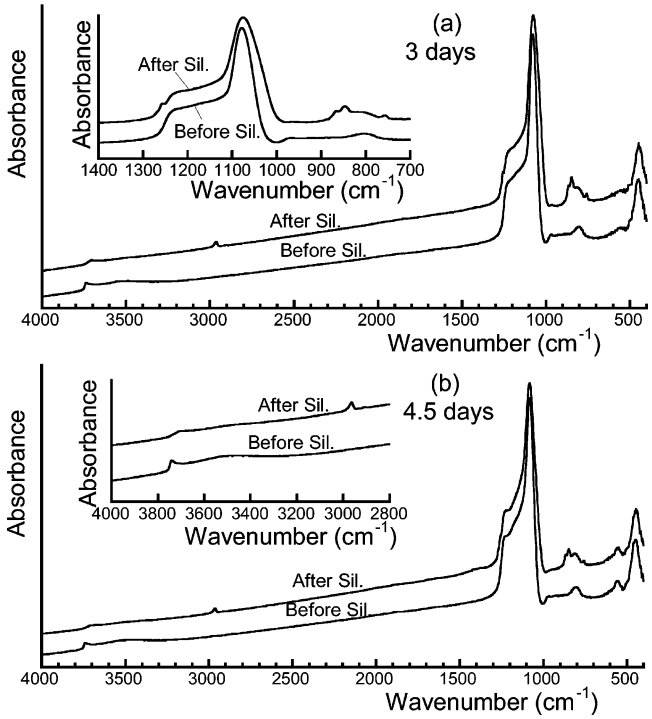

Figure 5. FT-IR spectra of spin-on Silicalite-1 films in the IR region of 4000−400 cm^{-1}. Films were prepared using Silicalite suspensions with different crystallization times: (a) 3 days and (b) 4.5 days. Spectra are zoomed in on the IR regions of 1400−700 cm^{-1} (inset in a) and 4000−2800 cm^{-1} (inset in b).

on various films silylated by the standard procedure at 450 °C. Silylated films were stored 2 weeks in a cleanroom environment (20 °C, air, 40% relative humidity) and subsequently heated to 450 °C for 30 min in the cleanroom. The water adsorption capacity rose by 1−2 vol % only. This confirms the durability of the hydrophobization treatment.

Fourier Transform Infrared Spectroscopy. Figure 5 shows the FT-IR spectra of the three spin-on Silicalite-1 films. FT-IR spectra of films prepared with long crystallized Silicalite-1 suspensions showed a more intense pentasil vibration at 550 cm^{-1} tantamount to higher zeolite crystallinity.[29] The 4.5 day film displayed a more intense external asymmetric stretching of the Si−O−Si bond (1220 cm^{-1}) relative to the internal asymmetric stretching (1110−1070 cm^{-1}).[28] However, there were no noticeable differences in the spectral range of silanols among the 3 and 4.5 day films. Stretching vibration bands of silanols are present at 3740 cm^{-1} (isolated silanols); 3700 cm^{-1} (geminal silanols or lattice defects); 3700−3450 cm^{-1} (H-bonded vicinal silanols and physisorbed water). The Si−OH stretching vibration is at 970 cm^{-1}.[16]

Figure 5 also shows the FT-IR spectra of the films after silylation. The incorporation of TMS groups altered the FT-IR spectra.[30] Bands at 750−875 cm^{-1} and 1250−1270 cm^{-1} are assigned to Si−CH_3 (see inset in Figure 5a). The internal asymmetric stretching of Si−O−Si bonds was broadened up to frequencies of 990 cm^{-1} (see inset in Figure 5a). This broadening results from the presence of Si−O−Si-$(CH_3)_3$ groups in which the Si−O−Si bond has a smaller angle and vibrates at lower wavenumber. Finally, at 2960 cm^{-1}, the asymmetric stretching of C−H_3 in TMS groups was visible.

TMS groups are incorporated by chemical substitution of the hydrogen atom in SiOH moieties.[20,31] A decrease of the intensity of the IR bands assigned to SiOH was observed indeed. The inset in Figure 5b, zoomed in on the frequencies of silanol vibrations, shows a decrease for all bands assigned to silanols and suggests that all the isolated silanols reacted with TMCS. There was no IR vibration band at 3740 cm^{-1} left. However, neither the geminal nor the vicinal silanols completely reacted with TMCS, as revealed by the residual IR vibration intensity at 3700−3450 cm^{-1}. Steric limitations must have hindered the reaction of TMCS with every geminal and vicinal silanol, as previously observed in other silica-based materials.[15,20]

TOF-SIMS. Figure 6 shows the carbon profiles that were determined using TOF-SIMS in two films before and after silylation. The carbon profile determination of the film with 3 days of crystallization before silylation was carried out successfully. However, on the film with 4.5 days of crystallization, the carbon profile could not be determined because the film did not withstand the ion bombardment. This was due to the poor mechanical properties of this film prepared using a long crystallized Silicalite-1 suspension, a feature that is known in the literature.[6,11] The differences in mechanical properties arise from the differences in the proportion of residual silica binder versus nanocrystals (94 wt % versus 69 wt % of residual silica of 3 and 4.5 days, respectively, see higher). The cohesion of the film with 4.5 days of crystallization was improved, however, after silylation. Silylation not only hydrophobized the films, but it also improved cohesion. It rendered the determination of the carbon profile possible (Figure 6).

The carbon profiles gave a clear image of the homogeneity of the hydrophobization along the depth of the film (Figure 6).

(29) Flanigen, E. M. *Zeolite Chemistry and Catalysis*; Rabo, J. A., Ed.; American Chemical Society: Washington, D.C., 1976; vol. 171, pp 80−117.

(30) Grill, A.; Neumayer, D. A. *J. Appl. Phys.* **2003**, *94*, 6697−6707.

(31) Nadiye-Tabbiruka, M. S.; Haynes, J. M. *Colloid Polym. Sci.* **1994**, *272*, 1602−1610.

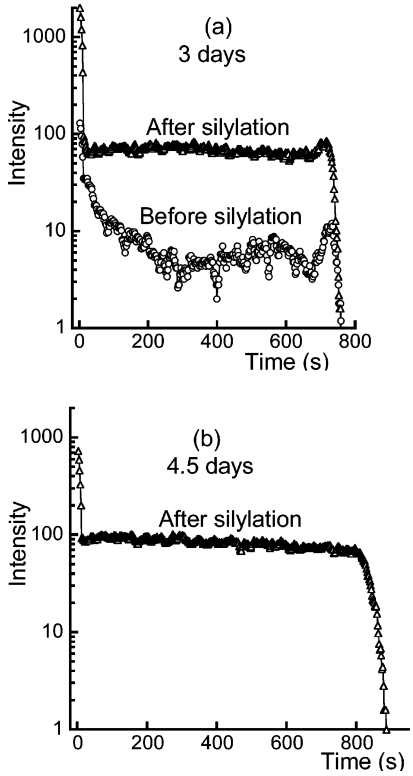

Figure 6. Carbon detected versus sputtering time in TOF-SIMS analysis of spin-on Silicalite-1 films before and after silylation. The films were prepared from suspensions with (a) 3 days and (b) 4.5 days crystallization.

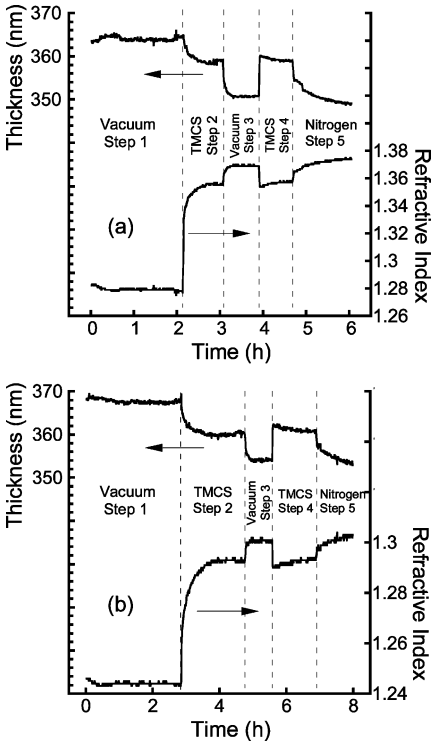

Figure 7. Evolution of the refractive index at 633 nm and of the thickness of spin-on Silicalite-1 films during the different steps of the silylation process. The films were prepared using Silicalite-1 crystallized for (a) 3 days and (b) 4.5 days.

Before TMCS treatment, some carbon was detected upon sputtering of the top layer. This carbon stemmed from a contamination of the film with organic molecules from the ambient upon storage. This interpretation was in line with the lower levels of carbon detection in deeper positions of the film. The detection of a small amount of carbon in the bulk of the film is attributed to organic template residues. The experiment on the silylated film revealed that the bulk of the film was silylated because there was constant and intense carbon release upon sputtering of the entire film. Note that bulk silylation was achieved even in the microporous film (3 days of Silicalite-1 crystallization). Pore blocking by TMS groups sometimes encountered in microporous materials was absent.[17,32] This demonstrates that the TMCS molecules can penetrate the internal volume of this PSZ film, yielding a homogeneous silylation. In the film prepared with 4.5 days crystallized Silicalite-1 suspension, the carbon release slightly decreased with sputtering time, showing that, in this case, the penetration of TMCS molecules was slightly hindered at deeper positions in the film.

In Situ Ellipsometry of the Silylation Reaction. The mechanism of silylation has been discussed in literature.[15,20,31,33] Prior to silylation with TMCS, a heating at 450 °C was performed to dehydrate and dehydroxylate the pore surface.[20,33] During this step, physisorbed water is desorbed, and siloxane bridges are formed:

$$\equiv SiOH\cdots H_2O \leftrightarrow \equiv SiOH + H_2O \quad (2)$$

$$\equiv SiOH\cdots HOSi\equiv \leftrightarrow \equiv SiOSi\equiv + H_2O \quad (3)$$

The extent of these reactions depends on the temperature.[20] At 450 °C, neither full dehydration nor full dehydroxylation is expected to occur, as these would need higher temperatures. For instance, mesoporous silica are fully dehydroxylated at temperatures above 900 °C.[34] The reaction of TMCS is known to occur preferentially with isolated silanols:[15,20]

$$\equiv SiOH + ClSi(CH_3)_3 \rightarrow \equiv SiOSi(CH_3)_3 + HCl \quad (4)$$

We performed in situ ellipsometry to reveal the kinetics of the silylation reaction on spin-on Silicalite-1 films. Figure 7 shows the refractive index and thickness of two films during the different steps of the silylation process. Initially, the films were in vacuo. The temperature was raised to 450 °C, and the sample was heated for 2−3 h (step 1). TMCS gas for silylation was introduced in the chamber (step 2). The refractive index of the films suddenly increased, followed by a more gradual increase until a plateau was reached when the reaction was finished. The reaction took 1−2 h. The film thickness evolved opposite to the refractive index. The increase in refractive index was attributed to the chemisorption of TMS and to the formation of a monolayer of TMS groups covalently linked to the pore surface. This modification seemed to have generated forces that shrunk the film, as the film thickness decreased by 1−2%. Physisorption of TMCS to explain the changes is unlikely because of the high temperature and the low TMCS pressure (2 mbar) used. The TMCS pressure was orders of magnitude smaller than the condensation pressure at 450 °C.

Nadiye-Tabbiruka et al. studied the kinetics of the TMCS reaction on a nonporous silica, Aerosil, and revealed that it follows

(32) O'Connor, C. T.; Möller, K. P.; Manstein, H. *J. Mol. Catal., A: Chem.* **2002**, *181*, 15−24.
(33) Denoyel, R.; Trens, P. *J. Phys. Chem.* **1995**, *99*, 3711−3714.
(34) Innocenzi, P.; Falcaro, P.; Grosso, D.; Babonneau, F. *J. Phys. Chem. B* **2003**, *107*, 4711−4717.

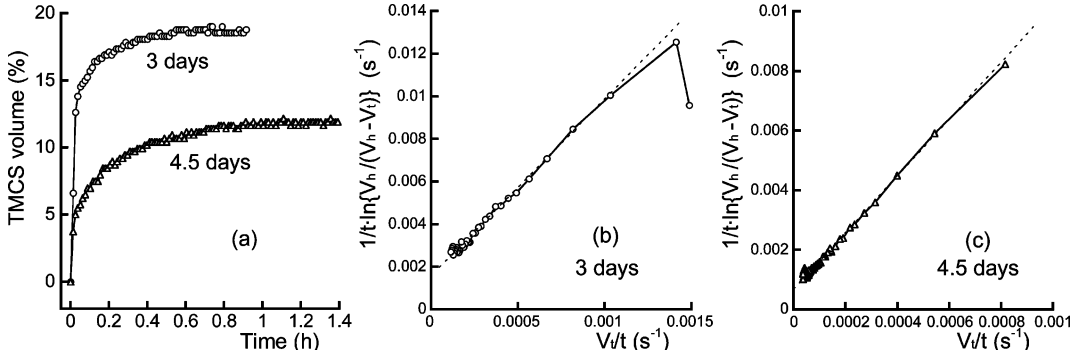

Figure 8. (a) TMS chemisorbed as a function of time during the reaction of TMCS on Silicalite-1 films at a pressure of 2 mbar; (b,c) plots to confirm the first-order kinetics inhibited by HCl. The films were prepared using Silicalite-1 suspensions crystallized during (b) 3 days and (c) 4.5 days.

first-order kinetics and is inhibited by the reaction product HCl.[26] The reaction kinetics can be expressed as

$$\left[\frac{1+b}{t}\right]\ln\left\{\frac{M_\infty}{M_\infty - M_t}\right\} - \frac{M_t \cdot b}{M_\infty \cdot t} = k_a \qquad (5)$$

where b is a composite coefficient, k_a is the rate coefficient, M_t is the mass of the gain during the TMCS reaction at time t, and M_∞ is the maximum mass gain. This kinetic model was evaluated on Aerosil silylation by plotting[26]

$$\frac{M_t}{t}$$

against

$$\frac{1}{t}\ln\left\{\frac{M_\infty}{M_\infty - M_t}\right\} \qquad (6)$$

Since a linear dependence is expected for both mass gain and volume gain, this kinetic model was evaluated for our present films by plotting

$$\frac{V_t}{t}$$

against

$$\frac{1}{t}\ln\left\{\frac{V_\infty}{V_\infty - V_t}\right\} \qquad (7)$$

where V_t is the volume fraction of the gain during TMCS reaction and V_∞ is the maximum volume fraction gain. Figure 8a shows the volume percent of TMS incorporated as a function of time during the first silylation step (step 2) on two films. In the calculations for the refractive index of the TMS monolayer, the value for liquid TMCS was taken, i.e., 1.387. The analysis of the reaction kinetics shown in Figure 8b and 8c confirmed the occurrence of first-order kinetics inhibited by the HCl product and suggested reaction microkinetics similar to those on Aerosil powder. Both the first-order reaction kinetics resembling those occurring in Aerosil together with the TOF-SIMS data suggesting uniform silylation reveal the effectiveness of the TMCS reaction in these spin-on Silicalite-1 films.

In situ ellipsometry technically presented some problems. In the first silylation step, the chamber was degassed to vacuum (step 3). Figure 7 shows an increase of refractive index accompanied by a decrease of thickness. Similar changes were also seen in the next degassing step (step 5). When TMCS was introduced for the second silylation reaction (step 4), both the refractive index and the thickness that were measured at the end of the first silylation step were recovered. This confirmed that the changes were due to technical problems. We attribute those artificial changes to a misalignment of the sample upon degassing and to inaccurate optical parameters used to account for the Si substrate. Additional tests revealed that, when the pressure was changed, the contact between the thermochuck and the sample was changed, which changed the sample temperature and the optical properties of the silicon support. The misalignment was, however, a more important problem than the temperature variation.

The refractive index of the film slightly increased during the second silylation step (step 4) compared to the first silylation step (step 2). Silylation was not fully achieved in the first silylation step. In the degassing operation in step 3, HCl inhibiting further reaction is desorbed. Similar observations were made elsewhere during silylation of nonporous silica.[31] This suggests that TMCS reaction can be optimized in a system where HCl reaction product is continuously evacuated.

Capacitance and Dielectric Constant. In view of the potential application of spin-on Silicalite-1 films in integrated circuits as low-k materials, we determined the dielectric constant for the silylated films via capacitance measurements. Before silylation, the capacitance measurement was not possible due to high leakage (a drop of 95% was observed in the applied alternating voltage, V_m). This high leakage revealed the hydrophilicity of the films. Even after water desorption by heating at 190 °C for 3 h in nitrogen gas, the high leakage was still present. After silylation, films exposed to ambient atmosphere also showed high leakage. Evacuation under nitrogen gas at 190 °C effectively lowered the leakage and permitted the capacitance measurement. The V_m drop was smaller than 3% in this case. The dielectric constant at 100 kHz was 4.4, 3.8, and 3.5 in dried silylated films prepared using Silicalite-1 suspensions crystallized for 3, 4, and 4.5 days, respectively.

Conclusions

The combination of FT-IR, EP, TOF-SIMS, and in situ ellipsometry provided detailed insight into the reaction of TMCS in spin-on Silicalite-1 films. Toluene adsorption capacities on the films revealed that the incorporation of TMS groups decreased the porosity by 26−56%, depending on the initial pore size distribution. The smaller the pores, the larger was the impact of the incorporation of TMS groups. Films with the narrowest pores presented the largest surface areas on which TMCS molecules

can react. Both the water adsorption capacity and the water contact angle confirmed that the films became hydrophobic. The reaction of TMCS took place on isolated silanols. The reaction of TMCS with geminal and vicinal silanols was sterically hindered. TOF-SIMS shows that the films were homogeneously modified. There were no important diffusion limitations for the reaction of TMCS in the films. The reaction kinetics obeyed first-order reaction kinetics inhibited by the HCl reaction product. Finally, capacitance−voltage measurement showed a reduction of the leakage as a consequence of the hydrophobization.

Acknowledgment. The authors acknowledge I. Callant and S. Esconjauregui for the silylation system and T. Conard for TOF-SIMS analysis. C.E.A.K. and J.A.M. acknowledge the Flemish government for a concerted research action (GOA).

LA800086Y